Distinct Symptom-Specific Treatment Targets for Circuit-Based Neuromodulation

Shan H. Siddiqi, M.D., Stephan F. Taylor, M.D., Danielle Cooke, B.S., Alvaro Pascual-Leone, M.D., Ph.D., Mark S. George, M.D., Michael D. Fox, M.D., Ph.D.

Objective: Treatment of different depression symptoms may require different brain stimulation targets with different underlying brain circuits. The authors sought to identify such targets, which could improve the efficacy of therapeutic brain stimulation and facilitate personalized therapy.

Methods: The authors retrospectively analyzed two independent cohorts of patients who received left prefrontal transcranial magnetic stimulation (TMS) for treatment of depression (discovery sample, N=30; active replication sample, N=81; sham replication sample, N=87). Each patient's TMS site was mapped to underlying brain circuits using functional connectivity MRI from a large connectome database (N=1,000). Circuits associated with improvement in each depression symptom were identified and then clustered based on similarity. The authors tested for reproducibility across data sets and whether symptom-specific targets derived from one data set could predict symptom improvement in the other independent cohort.

Results: The authors identified two distinct circuit targets effective for two discrete clusters of depressive symptoms. Dysphoric symptoms, such as sadness and anhedonia, responded best to stimulation of one circuit, while anxiety and somatic symptoms responded best to stimulation of a different circuit. These circuit maps were reproducible, predicted symptom improvement in independent patient cohorts, and were specific to active compared with sham stimulation. The maps predicted symptom improvement in an exploratory analysis of stimulation sites from 14 clinical TMS trials.

Conclusions: Distinct clusters of depressive symptoms responded better to different TMS targets across independent retrospective data sets. These symptom-specific targets can be prospectively tested in a randomized clinical trial. This data-driven approach for identifying symptom-specific targets may prove useful for other disorders and facilitate personalized neuromodulation therapy.

Am J Psychiatry 2020; 177:435–446; doi: 10.1176/appi.ajp.2019.19090915

Major depressive disorder is a heterogeneous syndrome with different clinical features that may not map to the same brain circuit (1). For instance, anhedonia and anxiety are both common symptoms of depression but are associated with different connectivity changes (2). Neuromodulation techniques such as transcranial magnetic stimulation (TMS) may begin to address this heterogeneity by targeting specific circuits to treat specific symptom clusters (3–5). However, it remains unknown whether stimulation of different circuits is associated with improvement in different depression symptoms.

In clinical practice, TMS targeting is usually based on scalp measurements, resulting in different patients receiving stimulation of different sites in the prefrontal cortex (6–8). This practice produces variance in the stimulation site, which can be linked to an underlying circuit by using the human connectome as a template (9). This variance has been used to retrospectively determine which stimulated circuit led to the best overall antidepressant response (10, 11). For example, patients who received stimulation at cortical sites connected to the subgenual cingulate have shown greater improvement in global depression scores (10, 11). This retrospective association has been used to optimize TMS targeting for recent prospective clinical trials (12–15).

However, because the previous work leading to this TMS target considered depression as a unitary measure (10, 11, 16), the optimized TMS target employed by recent prospective trials (12–15) may not be optimal for all symptom profiles. Here, we investigate multiple independent retrospective data sets to determine whether different symptom clusters respond better to stimulation of different brain circuits.

METHODS

Complete methodological details are presented in the online supplement.

See related features: **Editorial** *by Dr. Nestor and Dr. Blumberger (p. 373) and* **CME course** *(p. 469)*

Subjects and Data Collection

This study included two retrospective data sets of patients who received TMS for treatment-resistant depression (see Table S1 in the online supplement). All patients received high-frequency TMS using a standard figure-of-eight coil to the left dorsolateral prefrontal cortex (DLPFC) at 120% of resting motor threshold for 3–6 weeks. Stimulation sites were recorded on the patient's MRI and transformed to a standard brain atlas using the nonlinear transform function in SPM8. Further study details are delineated in the online supplement.

Discovery data set. Thirty patients received a 4- to 6-week naturalistic course of clinical TMS at the Berenson-Allen Center for Noninvasive Brain Stimulation in Boston. Treatment was targeted using the 5.5-cm rule. The stimulation site was recorded using stereotactic neuronavigation software (BrainSight, Rogue Research, Montreal). Outcomes included patients' self-reported responses on the Beck Depression Inventory (BDI) and a modified clinician-reported version of the 24-item Hamilton Depression Rating Scale (HAM-D). The BDI was treated as the primary outcome measure because responses were collected immediately before and after the clinical TMS course. The HAM-D was treated as a secondary outcome measure because responses were collected several months before or after treatment (mean pre- to post-treatment interval, 126 days), which may limit its reliability (17). The HAM-D was also modified for routine clinical use, including omission of three of the 24 items (genital/libido, paranoia, and insight). A subset of this cohort was previously used to predict global antidepressant response (10).

Replication data set. Eighty-one patients received active TMS, and 87 received sham treatment as part of the Optimization of TMS for the Treatment of Depression Study (6, 18). Patients received 3 weeks of blind TMS (active or sham), which was used as our primary endpoint. Some patients also received up to 3 additional weeks of open-label active TMS, which we used as a secondary endpoint. Treatment targeting was done using the 5-cm rule. The stimulation site was recorded by placing a vitamin E capsule over the site during an MRI scan. The primary outcome was the clinician-reported 28-item HAM-D, as in the original clinical trial (6). The self-reported Inventory of Depressive Symptomatology was also collected as a secondary outcome measure. This data set was used for replication rather than discovery to enable comparisons between active and sham treatment for the replication and because the method of recording the stimulation site may be less precise.

Statistical Testing

For permutation testing, each patient's symptom response was randomly reassigned to a different patient's stimulation site. After 10,000 iterations, solutions were considered significant if the outcome of interest was stronger for the real data than for 95% of random permutations. For correlation analyses, normality was assessed using the Shapiro-Wilk test, and nonnormally distributed data were rank-transformed.

Seed-Based Normative Connectivity Analysis

For each patient, the volume of brain tissue modulated by TMS was estimated using a previously specified model (10, 19) and using the above record of the stimulation coordinates in standard atlas space (Figure 1A). Normative connectivity of this stimulation site was computed using resting-state functional MRI (rsfMRI) data from a large connectome database (N=1,000) (20), as in past work (10). This method provides a highly reliable estimate of each stimulation site's expected connectivity profile (Figure 1B), enabling direct comparison of stimulated circuits and clinical changes (9–11, 16). Subject-specific functional connectivity data were available only for a subset of patients (N=30, out of 198) and thus were not incorporated into the model.

Correlation was computed between these stimulation site connectivity maps and the total change in each depression symptom across subjects. For example, in our discovery cohort, we performed correlations across 30 patients for each of the 21 symptoms measured by the BDI. At each voxel, this yielded a value representing the degree to which this voxel's connectivity to the stimulation site predicted efficacy for any given symptom. We refer to these voxel-wise maps as symptom-response maps (Figure 1C).
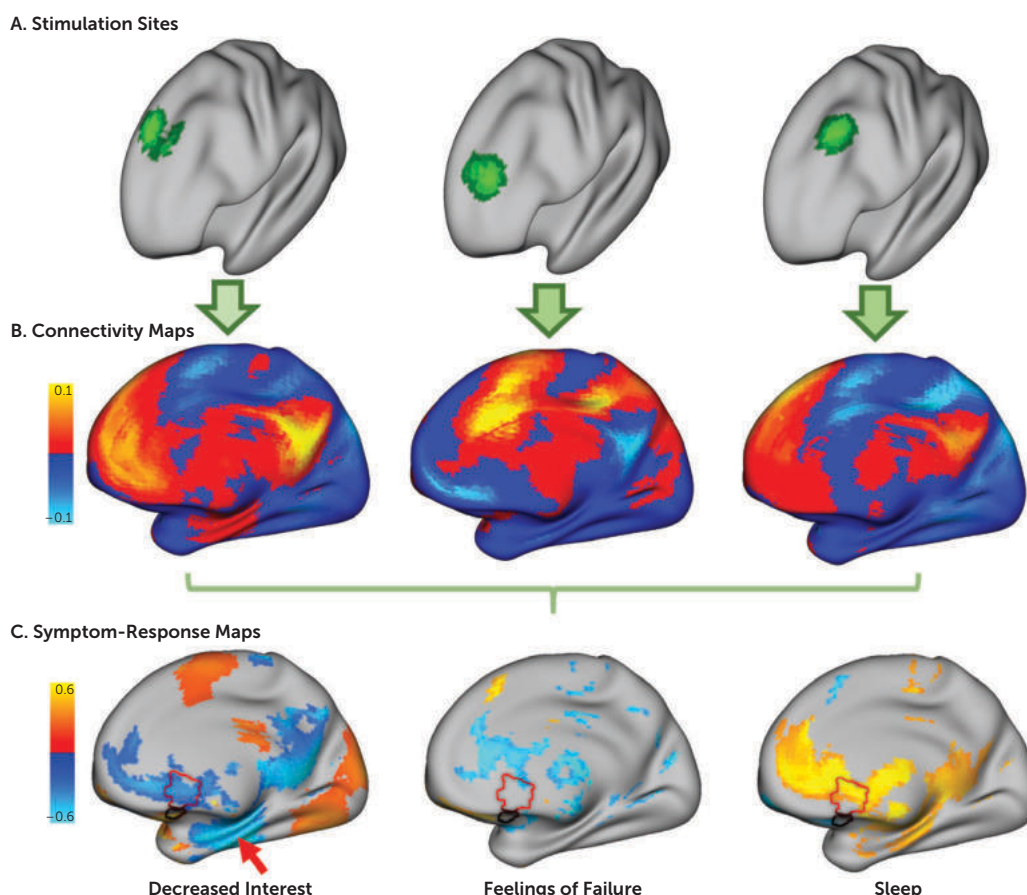
Clustering of Symptom-Response Maps

Because some symptom-response maps looked similar to one another, we classified similar maps into common clusters. The degree of similarity was quantified by calculating spatial correlation between each pair of symptom-response maps. Maps that were most similar to one another were grouped into clusters using Ward's hierarchical clustering method (21). The strength of clustering was evaluated using the gap statistic (22). Symptom-response maps within a cluster were averaged to generate a mean cluster-response map.

Control analyses were conducted to confirm that the results were not driven by the following factors:

1. Characteristics of the stimulation site alone: The analysis was repeated using baseline symptom severity (which should be unrelated to the stimulation site) rather than symptom improvement.
2. Covariance in symptom response alone: The analysis was repeated using symptom change alone, without considering the stimulation sites or their connectivity.
3. Random chance: The analysis was repeated after randomly assigning each patient's stimulation site to a different patient's clinical response.
4. Artificial binarization of a continuous distribution: We tested for normality of the real data (which should be nonnormal) using the Shapiro-Wilk test. We also used a permutation test to confirm that the strength of clustering (gap statistic) was stronger than would be expected by chance.
5. Influence of confounders: The analysis was repeated after controlling for the effect of age, sex, number of current antidepressant medications, and number of current psychotropic medications.

FIGURE 1. Identifying brain circuit targets for individual depressive symptoms in a study of symptom-specific treatment targets for circuit-based neuromodulation[a]

A. Stimulation Sites

B. Connectivity Maps

C. Symptom-Response Maps

Decreased Interest   Feelings of Failure   Sleep

[a] Patients receiving transcranial magnetic stimulation (TMS) for treatment of depression had their stimulation site recorded using MRI, revealing variability in the stimulation site across patients, as illustrated in the three patient examples in panel A. In panel B, the network of regions functionally connected to each patient's stimulation site was computed using a large normative connectome database (N=1,000). Connections correlated with improvement in individual depression symptoms across patients were identified, as illustrated with three symptom examples in panel C. Only some symptoms were related to connectivity with the subgenual cingulate (red outline), and the peak predictor was often in other regions, such as the hippocampus (red arrow). For illustrative purposes, these example maps are thresholded at uncorrected $p < 0.05$.

Reproducibility of Clustering Model

To assess reproducibility of our cluster-response maps, we repeated our clustering analysis for both symptom inventories in both data sets. Because "sadness" was a consistent question item across all symptom scales and data sets, we designated the cluster containing this symptom as cluster 1 and the remaining cluster as cluster 2. Discovery cluster-response maps were compared with replication cluster-response maps using spatial correlation, comparing cluster 1 to cluster 1 and cluster 2 to cluster 2. To assess significance, these values were compared with the spatial correlation generated from randomly permuted replication data. We also tested whether this replication was specific to active relative to sham stimulation. To confirm that the results were not driven by the choice of data set, we repeated our analysis using our discovery data to reproduce results from our replication data set. For all control analyses, we maintained the same definition of cluster 1 as the cluster containing "sadness."

Building a Targeting Atlas

For each voxel in the DLPFC, we used spatial correlations to compute the similarity between that voxel's connectivity and our two cluster-response maps. The DLPFC was defined as in Fox et al. (23). By definition, these maps reflect the symptomatic improvement expected after TMS to each voxel in the DLPFC. Because the two maps showed minimal overlap, we combined them into a single targeting atlas, which depicts targets expected to preferentially improve one of the two symptom clusters. We repeated this analysis for each data set independently.

Prediction of Relative Improvement in Symptoms Across Patients

The targeting atlas from one data set was used to predict preferential improvement in one of the two symptom clusters for each patient in the other independent data set. This prediction was based solely on the location of the patient's stimulation site on the independent targeting atlas.

Correlation was calculated between this predicted symptom response and the actual symptom response (the ratio of clinical improvement between the two clusters). Symptom ratios were rank-transformed because ratio analyses inherently show skewed distributions (24). This analysis was repeated for the sham arm of the replication data set. The significance of the interaction between the active and sham arms was assessed through permutation testing.

To confirm that the result was not influenced by features related to the normative connectome database (N=1,000), each cohort was also analyzed using an independent subset of this connectome database (N=500, for each).

Combining Both Data Sets

Symptom-response maps were generated for all symptoms across both data sets (active TMS only) and were clustered using the same methods as described above. Symptom-response maps in each cluster were averaged to form two overall cluster-response maps. These two cluster-response maps were used to build a composite targeting atlas following the methods described above.

Prediction of Relative Symptom Improvement Across Studies

A literature review was conducted to identify therapeutic TMS trials that used a focal figure-of-eight coil and measured distinct mood and anxiety rating scales, similar to previous work (16). Because individual symptom items were not reported in most studies, we used depression scales as a proxy for dysphoric symptoms and anxiety scales as a proxy for anxiosomatic symptoms. Each study's stimulation site was identified and converted to Montreal Neurological Institute (MNI) coordinates. The location of this stimulation site on the composite targeting atlas was used to predict the ratio of improvement between the two symptom domains. Correlation was calculated between this predicted symptom response ratio and the actual symptom response ratio. We also calculated the percentage of studies in which the model correctly predicted which symptom scale would improve preferentially. A single-proportion z test was used to determine whether this percentage was significantly different from 50%.

As a control, we repeated this analysis for trials of "deep" TMS that use a broader stimulation field than traditional figure-of-eight coils. We hypothesized that these nonfocal coils would stimulate both circuits, resulting in similar improvement in dysphoric and anxiosomatic symptoms. Specifically, we tested whether symptom response ratios showed greater variance in trials using focal TMS coils compared with nonfocal TMS coils.

RESULTS

Different Circuits for Different Symptom Clusters

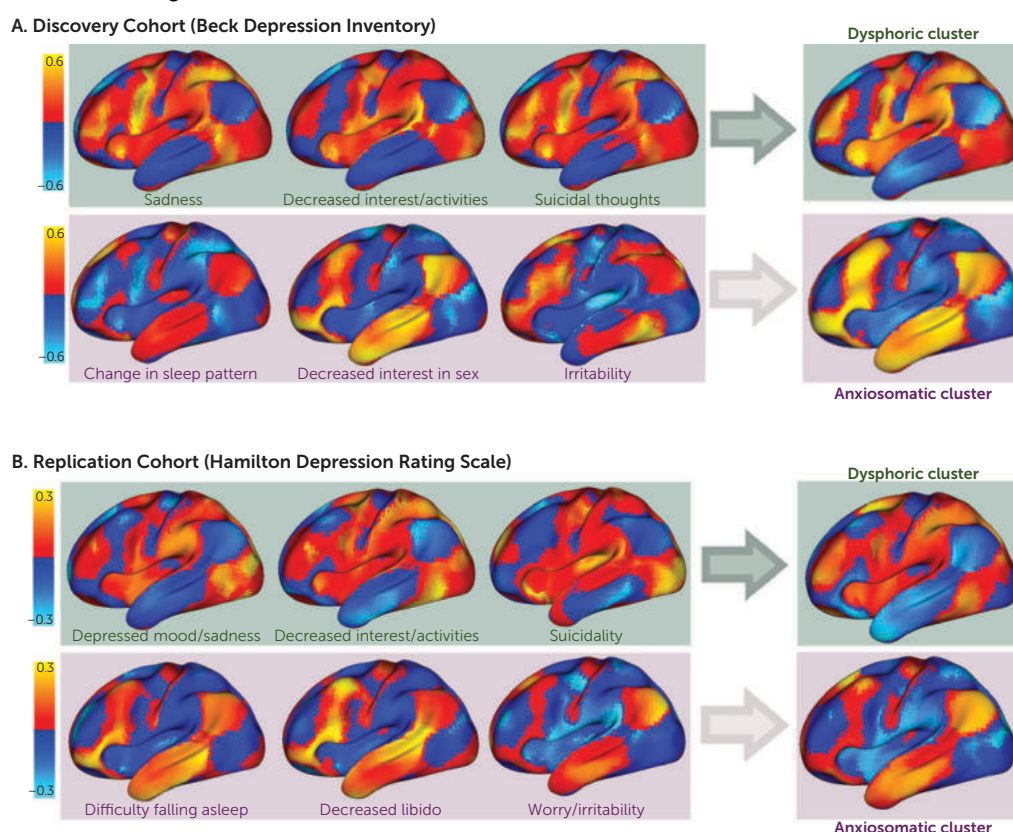Starting with our discovery data set and the patient-reported BDI, we computed 21 symptom-response maps that show connections with the stimulation site most correlated with improvement in each of the 21 symptoms (Figure 1C; see also Figure S1 in the online supplement). The correlation values in these maps were stronger than would be expected by chance (permutation test p<0.001). Although each symptom-response map was unique, the maps demonstrated one of two general topographic patterns (Figure 2; see also Figure S2 in the online supplement). An optimal two-cluster solution explained 73% of the variance as quantified by the gap statistic (see Figure S2 in the online supplement). One cluster included symptoms such as sadness, decreased interest, and suicidality, and a smaller cluster included symptoms such as irritability, sexual disinterest, and insomnia (Figure 2). For convenience, we refer to these clusters as "dysphoric" and "anxiosomatic," respectively.

We performed multiple control analyses to validate the clustering model (details are in Figure S2 in the online supplement). When this analysis was repeated using baseline symptom severity rather than symptom change, individual symptom-response maps showed weaker cross-correlation (unpaired t test, $p<1.0\times10^{-12}$) and did not result in a two-cluster solution. When this analysis was repeated using only symptom change, without consideration of the stimulation site, no clusters of covarying symptoms were identified. When both stimulation site and symptom change were included but randomly permuted, individual symptom-response maps showed weaker cross-correlation (p<0.005), and a two-cluster solution was identified less than half the time (42%). When a two-cluster solution was forced, it explained less variance than the two-cluster solution from the real data (p=0.02). Our two clusters did not result from artificial binarization of a normal distribution, as the real data deviated significantly from the normal distribution (p<0.05; see Figure S2 in the online supplement) and showed significantly stronger clustering than randomly permuted data (p<0.05; see Figure S2D in the online supplement). Finally, the maps were nearly identical when recomputed to control for age, sex, number of antidepressant medications, and number of psychotropic medications (spatial r>0.99).

Reproducible Clusters Across Symptom Scales and Independent Cohorts

An optimal two-cluster solution with similar topography was identified in our replication cohort, despite using a different symptom scale as the primary outcome measure (Figure 2). The use of secondary outcome measures for each data set (the HAM-D for the discovery sample and the Inventory of Depressive Symptomatology for the replication sample) produced nearly identical results (see Figures S4 and S5 in the online supplement). These cluster-response maps were more similar than would be expected by chance across different symptom scales (p<0.01) and across independent data sets (p<0.01). These results were not seen using the sham data (N=87), which produced a six-cluster solution. When forced to use a two-cluster solution, the sham data failed to match the discovery cohort as well as the active data (p<0.05). The reproducibility was unrelated to the choice of cohort, as the discovery cohort also

FIGURE 2. Connections correlated with improvement in individual depressive symptoms match one of two general patterns in a study of symptom-specific treatment targets for circuit-based neuromodulation[a]

A. Discovery Cohort (Beck Depression Inventory)

Sadness — Decreased interest/activities — Suicidal thoughts

Change in sleep pattern — Decreased interest in sex — Irritability

Dysphoric cluster

Anxiosomatic cluster

B. Replication Cohort (Hamilton Depression Rating Scale)

Depressed mood/sadness — Decreased interest/activities — Suicidality

Difficulty falling asleep — Decreased libido — Worry/irritability

Dysphoric cluster

Anxiosomatic cluster

[a] In our discovery cohort, shown in panel A, similar connections were correlated with improvement in certain symptoms assessed in the Beck Depression Inventory, such as sadness (item 1), decreased interest/activities (item 12), and suicidal thoughts (item 9). A distinct set of connections were correlated with improvement in other symptoms, such as change in sleep pattern (item 16), sexual interest (item 21), and irritability (item 17). Based on spatial similarity, our 21 individual symptom maps split into two distinct clusters, which we termed dysphoric and anxiosomatic. A similar two-cluster solution was identified in an independent replication cohort using a different symptom inventory (the 28-item Hamilton Depression Rating Scale), as shown in panel B. One cluster contained items such as depressed mood (item 1), decreased interest/activities (item 7), and suicidality (item 3), which we again termed dysphoric. A second cluster contained items such as difficulty falling asleep (item 4), decreased libido (item 14), and worry/irritability (item 10), which we again termed anxiosomatic. The dysphoric and anxiosomatic cluster maps (right panels) were highly reproducible across data sets (spatial $r=0.88$, $p<0.01$, 10^5 permutations).

significantly reproduced the maps derived from the replication cohort ($p<0.01$).

## Identification of Potential Treatment Targets in Each Cohort

The maps described above represent connections specific to "antidysphoric" or "antianxiosomatic" TMS sites in the discovery (Figure 2A) and replication (Figure 2B) cohorts. To identify TMS targets connected to these regions, we used spatial correlations to compare each voxel's connectivity profile with each dysphoric and anxiosomatic cluster map. This revealed an atlas of potential antidysphoric and antianxiosomatic TMS sites (Figure 3A and 3B). For each cohort, the antidysphoric and antianxiosomatic atlases were combined into a targeting atlas (Figure 3C) to predict relative improvement in dysphoric and anxiosomatic symptoms in the other cohort (examples shown in Figure 4A).

Validation Across Patients

We tested whether we could predict clinical improvement in one patient cohort using the targeting atlas derived from the other independent cohort (Figure 4). Starting with the stimulation sites from our discovery cohort, we found that the location of each patient's stimulation site on the targeting atlas derived from our replication cohort predicted the ratio of dysphoric to anxiosomatic symptom improvement (N=30, $r_s=0.69$, $p<10^{-4}$). This prediction was significantly stronger for the real discovery data than for randomly permuted discovery data ($p<10^{-3}$).

Similarly, we found that the location of each patient's stimulation site in our replication cohort on the targeting atlas derived from our discovery cohort could predict clinical response at both the 3-week time point (N=81, $r_s=0.47$, $p<10^{-5}$) and after the full course of treatment (N=81, $r_s=0.52$, $p<10^{-6}$). This prediction was significantly stronger in the active arm of the replication data set than in the sham arm of the same data set ($p<10^{-3}$).

FIGURE 3. Distinct circuit-based transcranial magnetic stimulation (TMS) targets for dysphoric and anxiosomatic symptoms in a study of symptom-specific treatment targets for circuit-based neuromodulation[a]
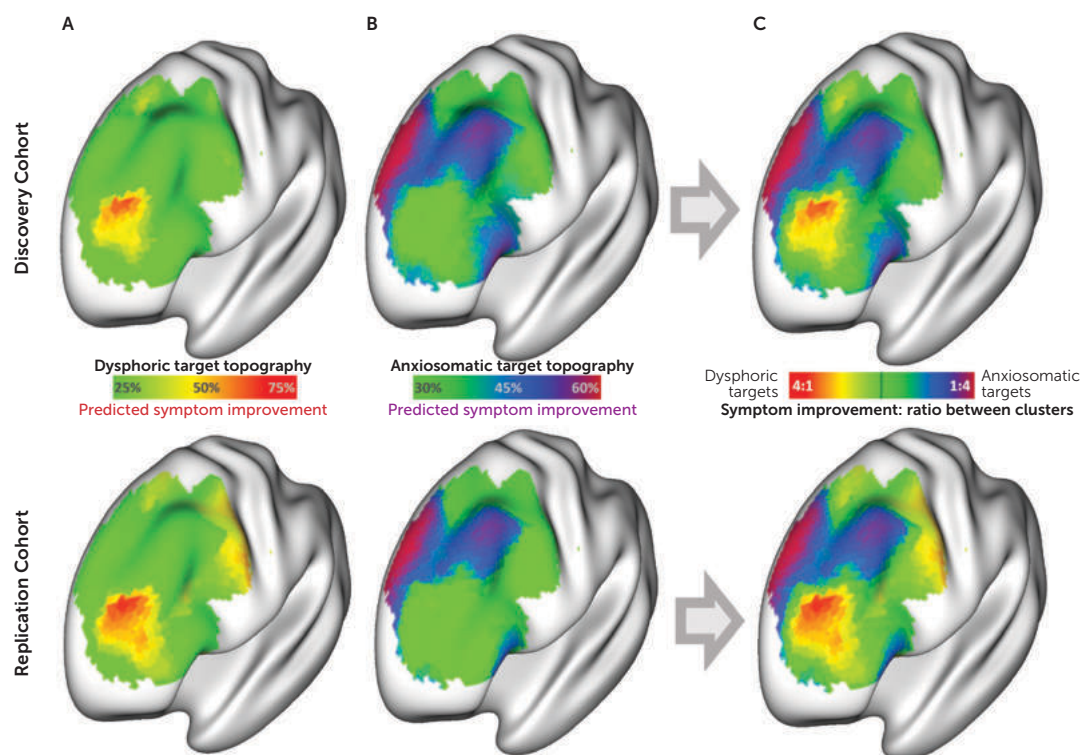
[a] In both the discovery and replication cohorts, "optimal" TMS targets were identified at voxels whose connectivity profile most closely matched our dysphoric cluster map (panel A) and our anxiosomatic cluster map (panel B). For each data set, these maps were combined to identify a targeting atlas for predicting relative improvement in dysphoric and anxiosomatic symptoms (panel C).

Results were unchanged when controlling for baseline symptom severity or when using an independent connectome data set ($2 \times N=500$) to compute the discovery and replication targeting atlases.

Combining Both Data Sets

All symptom-response maps across both data sets (active arm only) and both symptom scales were combined into a single large clustering analysis. This model again identified distinct dysphoric and anxiosomatic clusters. The symptom-response maps in each cluster were averaged to create combined cluster maps across data sets.

These cluster maps were largely the inverse of one another (spatial $r=-0.85$), but this result was not mandated by the clustering analysis, as permuted data with a forced two-cluster solution showed a significantly weaker spatial correlation (mean $r=-0.07$, $p<0.05$). Furthermore, some regions were not inverted and were common to both clusters, including the left DLPFC, the right orbitofrontal cortex, the periaqueductal gray, and the left anterior insula (see Figure S6 in the online supplement). Because connectivity may differ in the included patient population, we repeated this final clustering analysis using a smaller connectome database of patients who received rsfMRI scans before a clinical course of TMS for major depression (N=38). This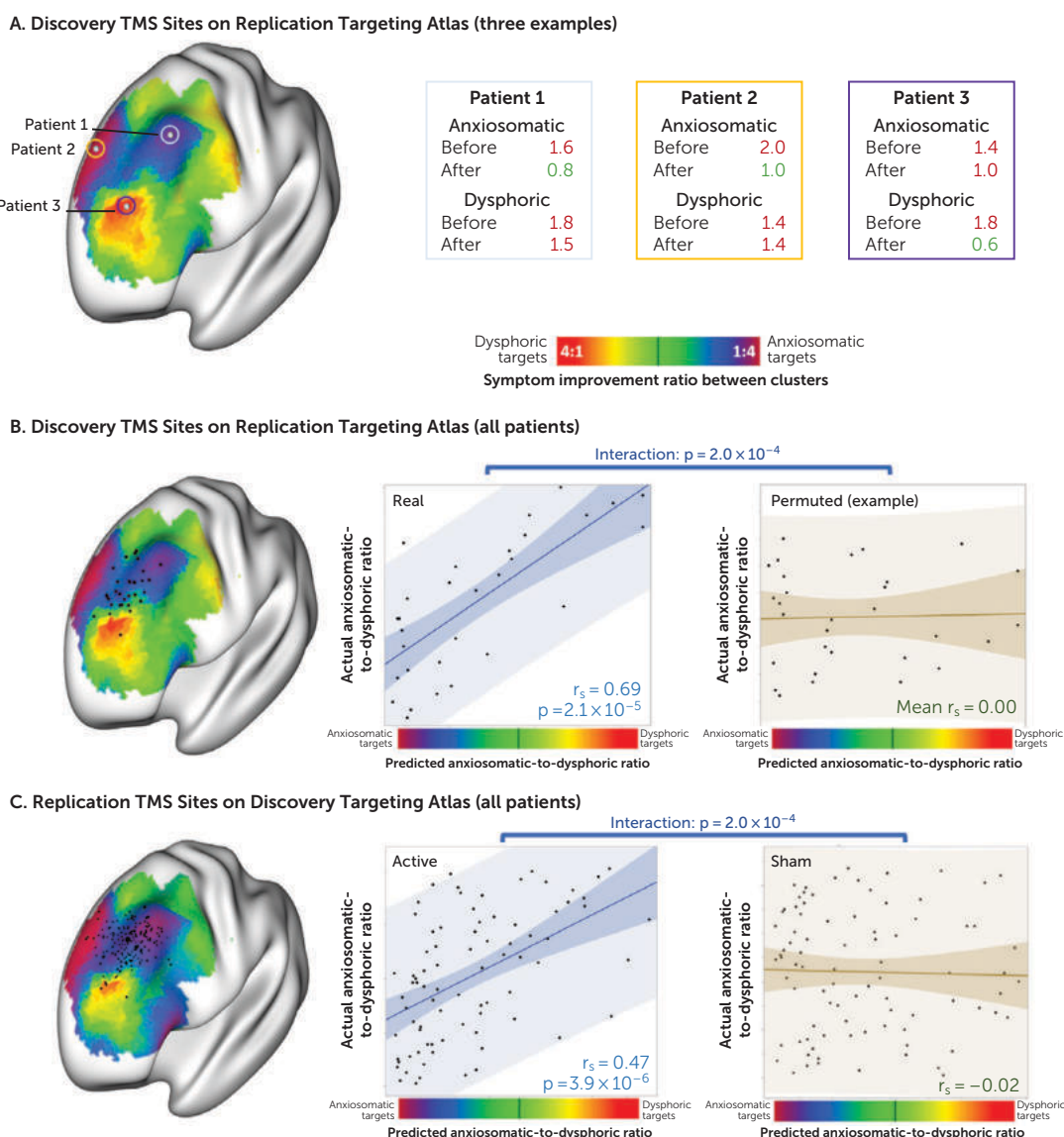 analysis revealed a solution similar to that derived from our larger normative connectome database (see Figure S7 in the online supplement).

These overall antidysphoric and antianxiosomatic maps were combined into a single composite targeting atlas following the same procedure as described above (Figure 5A–C). The peak dysphoric target was at MNI coordinates [−32, 44, 34], close to the "anti-subgenual" target used in recent TMS trials (Figure 5A) (12, 13). This dysphoric target lies at the intersection of Brodmann's areas 9, 10, and 46 and is part of a brain network variably referred to as the ventral attention, salience, and cingulo-opercular network (see Figure S8 in the online supplement) (20).

Within the left DLPFC, the peak anxiosomatic target was at MNI coordinates [−37, 22, 54], close to the 5-cm target used in early TMS clinical trials for depression (6, 25). There was also an anxiosomatic target in the dorso-medial prefrontal cortex at MNI coordinates [18, 37, 55], close to the target used in TMS trials for eating disorders, obsessive-compulsive disorder (OCD), and the anxiety/insomnia biotype of major depression (Figure 5B) (2, 26–28). Both anxiosomatic targets fall within Brodmann's area 8, part of the default mode network (see Figure S8 in the online supplement) (20).

A recent lesion network mapping study identified a specific DLPFC region with increased connectivity to lesion

FIGURE 4. Location of stimulation site and improvement in symptoms in individual patients in a study of symptom-specific treatment targets for circuit-based neuromodulation[a]

A. Discovery TMS Sites on Replication Targeting Atlas (three examples)

Patient 1		Patient 2		Patient 3	
Anxiosomatic		**Anxiosomatic**		**Anxiosomatic**	
Before	1.6	Before	2.0	Before	1.4
After	0.8	After	1.0	After	1.0
Dysphoric		**Dysphoric**		**Dysphoric**	
Before	1.8	Before	1.4	Before	1.8
After	1.5	After	1.4	After	0.6

Dysphoric targets 4:1 — 1:4 Anxiosomatic targets
Symptom improvement ratio between clusters

B. Discovery TMS Sites on Replication Targeting Atlas (all patients)

Interaction: $p = 2.0 \times 10^{-4}$

Real — Actual anxiosomatic-to-dysphoric ratio — $r_s = 0.69$ $p = 2.1 \times 10^{-5}$

Permuted (example) — Actual anxiosomatic-to-dysphoric ratio — Mean $r_s = 0.00$

Anxiosomatic targets — Dysphoric targets — **Predicted anxiosomatic-to-dysphoric ratio**

C. Replication TMS Sites on Discovery Targeting Atlas (all patients)

Interaction: $p = 2.0 \times 10^{-4}$

Active — Actual anxiosomatic-to-dysphoric ratio — $r_s = 0.47$ $p = 3.9 \times 10^{-6}$

Sham — Actual anxiosomatic-to-dysphoric ratio — $r_s = -0.02$

Anxiosomatic targets — Dysphoric targets — **Predicted anxiosomatic-to-dysphoric ratio**

[a] Three exemplary stimulation sites from the discovery cohort in relation to a targeting atlas generated from the replication cohort are shown in panel A. Patients who received stimulation at anxiosomatic sites showed greater improvement in anxiosomatic symptoms (e.g., patients 1 and 2), while patients who received stimulation at dysphoric sites showed greater improvement in dysphoric symptoms (e.g., patient 3). For each cohort, stimulation sites from each individual patient (black dots) are shown in panel B overlaid on a transcranial magnetic stimulation (TMS) targeting atlas generated from the other cohort. Across patients who received active TMS, the location of the stimulation site on the targeting atlas was correlated with improvement in dysphoric, relative to anxiosomatic, symptoms, as shown in panel C. This relationship was not seen with randomly permuted data or in patients who received sham TMS.

locations associated with overall depression scores. This region falls at the intersection of our dysphoric and anxiosomatic circuit targets (see Figure S8C in the online supplement) (29).

Prediction of Relative Symptom Improvement Across Studies

In an exploratory analysis, we tested whether our composite targeting atlas could predict variability in past TMS clinical trials. In addition to the two data sets described above, we identified 12 studies (see Table S4 in the online supplement)

reporting distinct depression and anxiety scales after at least 3 weeks of high-frequency focal TMS (6, 12, 14, 26–28, 30–36). Six studies stimulated relatively dysphoric sites, and eight studies stimulated relatively anxiosomatic sites (Figure 5C). Our prediction was correct in 13 of 14 studies ($p < 10^{-3}$, single proportion z test). Relative improvement in depression as opposed to anxiety was strongly correlated with the predicted improvement based on the location of each stimulation site on our targeting atlas (r=0.88, $p < 10^{-4}$) (Figure 5D).

Of note, the seminal clinical trial by O'Reardon et al. (25) was excluded because it lacked anxiosomatic scales,

FIGURE 5. The combined targeting atlas and prediction of improvement in symptoms across previous trials involving transcranial magnetic stimulation (TMS)[a]
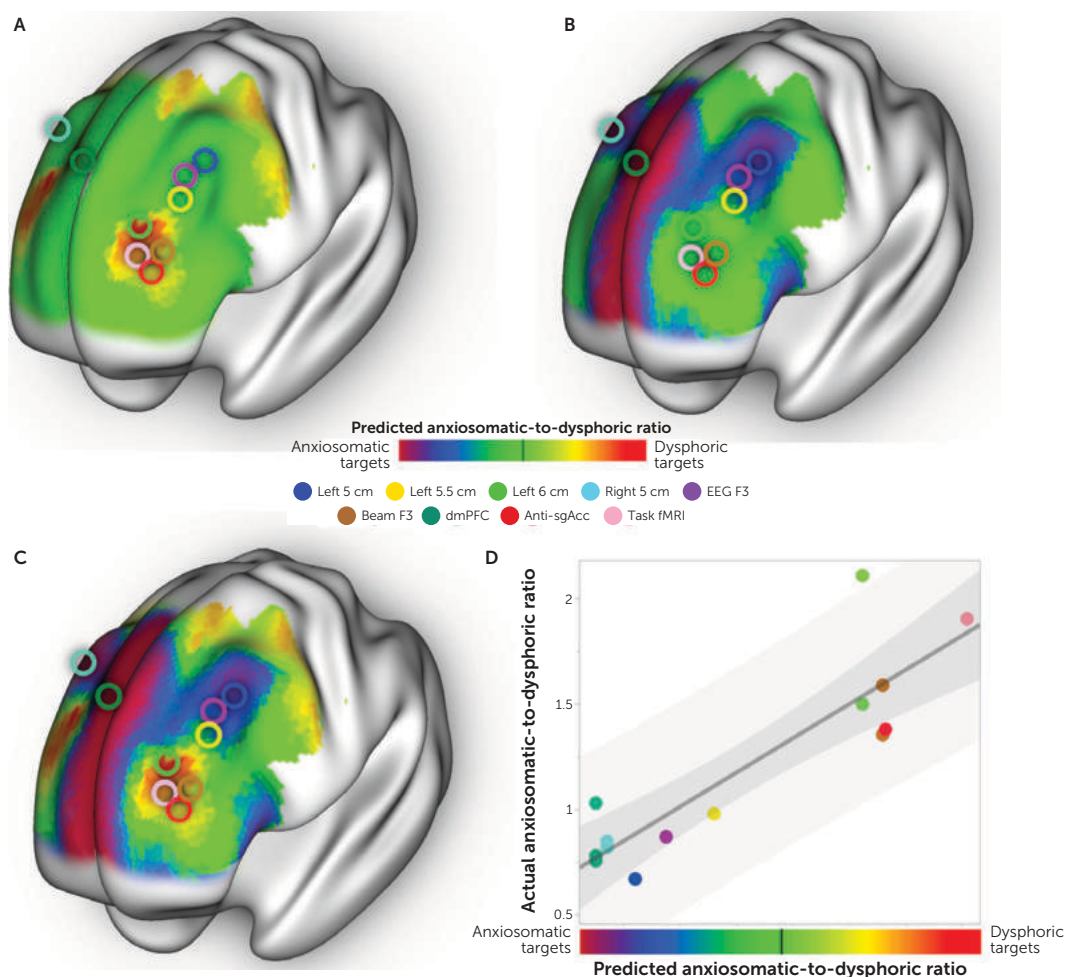
[a] We identified 14 TMS clinical trials (listed in Table S4 in the online supplement) employing nine different prefrontal treatment targets, which are depicted here as open circles. These previous treatment targets are shown overlaid on our targeting atlas for dysphoric symptoms (panel A), for anxiosomatic symptoms (panel B), and for the ratio of dysphoric to anxiosomatic symptoms (panel C) derived from combining our two retrospective TMS data sets. As shown in panel D, the ratio of anxiosomatic to dysphoric symptom improvement in these trials was correlated with the position of the trial's stimulation site on the targeting atlas. dmPFC=dorsomedial prefrontal cortex; fMRI=functional MRI; sgACC=subgenual anterior cingulate cortex.

but it was consistent with our prediction for the 5-cm stimulation site. Specifically, the study reported greater improvement in scores on the HAM-D, a multidimensional scale that also incorporates anxiety and somatic symptoms (37), than on the Montgomery-Åsberg Depression Rating Scale, a unidimensional metric more heavily focused on dysphoric symptoms (37).

As a control, we identified six additional studies of nonfocal "deep" TMS, which stimulates a broad field covering all the stimulation targets identified in this study (38–44). We hypothesized that nonfocal TMS would modulate symptoms nonspecifically, leading to a uniform depression-to-anxiety ratio across studies. Indeed, the depression-to-anxiety ratio showed significantly less variance with nonfocal TMS (range=0.94–1.19, SD=0.10)

than with focal TMS (range=0.67–1.94, SD=0.38) (p<0.01, F test for equal variances).

DISCUSSION

Despite long-standing recognition that patients with major depressive disorder can have very different symptoms (45), the field has yet to reach a consensus subclassification. Traditional classifications have contrasted "melancholic" with "agitated" or "atypical" subtypes, while contemporary classifications have contrasted "core" symptom clusters with "sleep" and "anxiety" clusters (46, 47). Some studies have proposed distinct circuit-based "biotypes" associated with distinct clinical features, such as anhedonia, anxiety, or rumination (1, 2). However, despite these

advances, subtyping based on symptoms and biological correlates has yet to improve treatment outcomes (48).

Here, we took a reverse approach toward therapeutically oriented biotyping. Rather than identifying biotypes and then searching for therapeutic relevance, we started with therapeutic response to an anatomically targeted intervention. This intrinsically links therapeutic specificity with anatomical specificity and identification of treatment targets. Thus, we were able to simultaneously identify two symptom clusters that respond to two distinct neuroanatomical treatment targets. We labeled these response patterns as dysphoric and anxiosomatic to prevent confusion with existing diagnostic classifications. Although these cluster labels and their constituent symptoms may be refined in future work, our analyses confirm that different patterns of response are associated with different TMS targets. These clusters were not explained by random chance or by anatomical features inherent to the stimulation sites. The clusters were also not driven by covariance in symptom improvement alone, suggesting that the anatomical contrast greatly increases our power to detect symptom-specific efficacy.

At the individual patient level, our targets predicted clinical improvement across independent data sets, suggesting potential clinical utility. At the population level, our targets explained variance in past TMS clinical trials. This exploratory population-level analysis is somewhat limited by inclusion of anxiosomatic symptoms in most depression scales, which may introduce noise into the analysis. Despite this noise, our model predicted significant variance in past clinical trials, suggesting that this approach may be useful for assessing future clinical trial outcomes.

Our finding of distinct dysphoric and anxiosomatic circuit targets is consistent with recent work identifying anhedonia/psychomotor retardation and anxiety/insomnia as distinct biotypes in major depressive disorder (2). In this study, the anxiety/insomnia biotype was preferentially responsive to dorsomedial prefrontal TMS (2), which aligns with our anxiosomatic target (Figure 5). Our work is also consistent with recent studies showing that anhedonia was preferentially responsive to DLPFC stimulation sites that align with our dysphoric target (49–51).

Strengths of our study include an empirical data-driven approach independent of a priori models of depression or symptom localization (52), replication across independent cohorts with very different study characteristics, specificity to active versus sham TMS, permutation-based statistics to ensure valid clustering (53), and direct therapeutic relevance for guiding future trials. The primary weakness of our study is that both of our independent cohorts were retrospective. This was not a clinical trial. The goal of our study was to derive reproducible symptom-specific TMS targets. We achieved this goal, but the clinical utility of the identified targets and symptom clusters remains to be prospectively tested in a randomized clinical trial.

It is worth noting that not all symptom-response maps were equally consistent across data sets and symptom scales. Some symptoms, such as sadness, decreased interest/activities, suicidality, guilt, and hopelessness/pessimism, were consistently part of the dysphoric cluster. Symptoms such as insomnia and sexual dysfunction were consistently part of the anxiosomatic cluster, with the exception of the HAM-D in the discovery cohort. This HAM-D score may be less reliable because it was collected at a clinical appointment months before the start of TMS and excluded questions about sexual function. Alternatively, reduced consistency in our anxiosomatic cluster may be due to greater heterogeneity in the interpretation of anxiosomatic relative to dysphoric question items (54) or the fact that our study focused on patients with major depression, who will have an overrepresentation of dysphoric relative to anxiosomatic symptoms. Further work using a truly transdiagnostic patient cohort with deeper phenotyping (including a discrete anxiety scale) may enable more definitive characterization and subclassification of these provisional clusters.

Additional limitations of our study that may be improved in future work include individualization of TMS and functional connectivity models. TMS electric field modeling may help to incorporate additional variables, such as angle and rotation of the TMS coil, stimulation intensity, and patient-specific anatomy (55). Individualized rsfMRI data may further enable modeling of interindividual variability in brain circuit topography (56). However, these specialized tools may be difficult to implement in clinical practice. Electric field modeling can require a high-performance computing cluster (55), and reliable individualized functional connectivity measurements may require hours of specialized MRI scanning (56). The added value of these advances needs to be determined and weighed against the additional cost and complexity for guiding clinical intervention.

An important question is whether our results are biased by factors that are mandated by the analysis. For example, a recent connectivity-based biotyping study of major depression may have artificially clustered a continuous phenomenon (53). We ensured that our clustering model was based on a parameter that did not follow a continuous distribution and that randomly permuted data showed significantly weaker clustering. Similarly, because the human brain is divided into two large anti-correlated networks (57), it is possible that any analysis would identify two symptom clusters that map to these two networks. We ensured that this was not the case by showing that randomly permuted data and sham TMS data both failed to yield a similar two-cluster solution. Finally, because we first clustered both data sets and then predicted the ratio of symptom improvement using those same clusters, the analysis may seem circular. However, the ratio of symptom improvement for each data set was predicted on the basis of a targeting atlas derived from an independent data set, mitigating this concern. Furthermore, a biased or circular analysis would have produced similar results for the sham replication cohort, which was analyzed in the same way as the active replication cohort but failed to produce

similar results. Randomly permuted data also failed to produce similar results when analyzed in the same manner.

Our findings in this study may help facilitate personalized medicine, targeting patient-specific symptoms based on neuromodulation of specific brain circuits. At a minimum, this work supports distinct assessment of dysphoric and anxiosomatic symptoms for patients receiving clinical TMS for depression. This may enable patient-specific selection and adjustment of treatment targets. For instance, residual anxiosomatic symptoms may be targeted in patients who initially show improvement only in dysphoric symptoms. Anxiosomatic sites may also be chosen for certain patients with comorbid anxiety disorders, OCD, posttraumatic stress disorder (PTSD), or somatoform disorders.

This work may also inform the design of clinical trials in neuromodulation for disorders with predominantly dysphoric versus anxiosomatic symptoms. Existing neuromodulation trials have employed broad symptom scales (6, 12, 25, 58–60) that may be insensitive to symptom-specific effects, potentially leading to false negative results (14, 35, 61, 62). For instance, a recent trial failed to demonstrate antidepressant efficacy of TMS in part because it appeared to exacerbate comorbid PTSD symptoms (14). Our results suggest that the 6-cm TMS target employed in this study would be expected to improve dysphoric but not anxiosomatic symptoms, offering a potential explanation for these results. Future neuromodulation trials may benefit from an assessment tool that clearly discriminates between different patterns of response.

Finally, our results may be relevant beyond the field of TMS and depression. For instance, different symptoms of Parkinson's disease respond to different deep brain stimulation (DBS) targets. Tremor (but not other symptoms) responds well to thalamic stimulation, while dyskinesias respond best to stimulation of the globus pallidus (63). Given evidence that symptom improvement depends on connectivity between the DBS site and other brain regions (64), distinct circuit targets for specific symptoms of Parkinson's disease could potentially be derived using the method outlined in this study.

In summary, we describe a novel approach for harnessing a targeted intervention to distinguish anatomical-behavioral relationships that previously remained elusive. This approach provides a framework for empirical derivation of symptom-specific treatment targets that may prove useful in other disorders and for other types of focal neuromodulation.

AUTHOR AND ARTICLE INFORMATION

Department of Psychiatry (Siddiqi) and Department of Neurology (Pascual-Leone, Fox), Harvard Medical School, Boston; Berenson-Allen Center for Noninvasive Brain Stimulation (Siddiqi, Cooke, Fox), and Cognitive Neurology Unit, Department of Neurology (Siddiqi), Beth Israel Deaconess Medical Center, Boston; Division of Neurotherapeutics, McLean Hospital, Belmont, Mass. (Siddiqi); Department of Psychiatry, Washington University School of Medicine, St. Louis (Siddiqi); Center for Neuroscience and Regenerative Medicine, Uniformed Services University of the Health Sciences, Bethesda, Md. (Siddiqi); Department of Psychiatry, University of Michigan School of Medicine, Ann Arbor (Taylor); Hinda and Arthur Marcus Institute for Aging Research and Center for Memory Health, Hebrew SeniorLife, Boston (Pascual-Leone); Guttmann Institute, Autonomous University of Barcelona, Barcelona, Spain (Pascual-Leone); Brain Stimulation Lab, Department of Psychiatry, Medical University of South Carolina, Charleston (George); Ralph H. Johnson VA Medical Center, Charleston, S.C. (George); Department of Neurology, Massachusetts General Hospital, Boston (Fox); Athinoula A. Martinos Center for Biomedical Imaging, Charlestown, Mass. (Fox).

Send correspondence to Dr. Siddiqi (shan.siddiqi@mgh.harvard.edu).

REFERENCES

1. Williams LM: Defining biotypes for depression and anxiety based on large-scale circuit dysfunction: a theoretical review of the evidence and future directions for clinical translation. Depress Anxiety 2017; 34:9–24
2. Drysdale AT, Grosenick L, Downar J, et al: Resting-state connectivity biomarkers define neurophysiological subtypes of depression. Nat Med 2017; 23:28–38
3. Philip NS, Barredo J, van 't Wout-Frank M, et al: Network mechanisms of clinical response to transcranial magnetic stimulation in posttraumatic stress disorder and major depressive disorder. Biol Psychiatry 2018; 83:263–272
4. Liston C, Chen AC, Zebley BD, et al: Default mode network mechanisms of transcranial magnetic stimulation in depression. Biol Psychiatry 2014; 76:517–526
5. Mirza S, Yazdani U, Dewey Iii R, et al: Comparison of globus pallidus interna and subthalamic nucleus in deep brain stimulation for parkinson disease: an institutional experience and review. Parkinsons Dis 2017; 2017:3410820
6. George MS, Lisanby SH, Avery D, et al: Daily left prefrontal transcranial magnetic stimulation therapy for major depressive disorder: a sham-controlled randomized trial. Arch Gen Psychiatry 2010; 67:507–516
7. George MS, Taylor JJ, Short EB: The expanding evidence base for rTMS treatment of depression. Curr Opin Psychiatry 2013; 26:13–18
8. Perera T, George MS, Grammer G, et al: The Clinical TMS Society consensus review and treatment recommendations for TMS therapy for major depressive disorder. Brain Stimul 2016; 9:336–346
9. Fox MD: Mapping symptoms to brain networks with the human connectome. N Engl J Med 2018; 379:2237–2245
10. Weigand A, Horn A, Caballero R, et al: Prospective validation that subgenual connectivity predicts antidepressant efficacy of transcranial magnetic stimulation sites. Biol Psychiatry 2018; 84:28–37
11. Cash RFH, Zalesky A, Thomson RH, et al: Subgenual functional connectivity predicts antidepressant treatment response to transcranial magnetic stimulation: independent validation and evaluation of personalization. Biol Psychiatry 2019; 86:e5–e7
12. Blumberger DM, Vila-Rodriguez F, Thorpe KE, et al: Effectiveness of theta burst versus high-frequency repetitive transcranial magnetic stimulation in patients with depression (THREE-D): a randomised non-inferiority trial. Lancet 2018; 391:1683–1692
13. Williams NR, Sudheimer KD, Bentzley BS, et al: High-dose spaced theta-burst TMS as a rapid-acting antidepressant in highly refractory depression. Brain 2018; 141:e18

14. Yesavage JA, Fairchild JK, Mi Z, et al: Effect of repetitive transcranial magnetic stimulation on treatment-resistant major depression in US veterans: a randomized clinical trial. JAMA Psychiatry 2018; 75: 884–893

15. Siddiqi SH, Trapp NT, Hacker CD, et al: Repetitive transcranial magnetic stimulation with resting-state network targeting for treatment-resistant depression in traumatic brain injury: a randomized, controlled, double-blinded pilot study. J Neurotrauma 2019; 36:1361–1374

16. Fox MD, Buckner RL, White MP, et al: Efficacy of transcranial magnetic stimulation targets for depression is related to intrinsic functional connectivity with the subgenual cingulate. Biol Psychiatry 2012; 72:595–603

17. Trajković G, Starčević V, Latas M, et al: Reliability of the Hamilton Rating Scale for Depression: a meta-analysis over a period of 49 years. Psychiatry Res 2011; 189:1–9

18. Johnson KA, Baig M, Ramsey D, et al: Prefrontal rTMS for treating depression: location and intensity results from the OPT-TMS multi-site clinical trial. Brain Stimul 2013; 6:108–117

19. Fox MD, Buckner RL, Liu H, et al: Resting-state networks link invasive and noninvasive brain stimulation across diverse psychiatric and neurological diseases. Proc Natl Acad Sci USA 2014; 111:E4367–E4375

20. Yeo BT, Krienen FM, Sepulcre J, et al: The organization of the human cerebral cortex estimated by intrinsic functional connectivity. J Neurophysiol 2011; 106:1125–1165

21. Murtagh F, Legendre P: Ward's hierarchical agglomerative clustering method: which algorithms implement Ward's criterion? J Classif 2014; 31:274–295

22. Tibshirani R, Walther G, Hastie T: Estimating the number of clusters in a data set via the gap statistic. J R Stat Soc Series B Stat Methodol 2001; 63:411–423

23. Fox MD, Liu H, Pascual-Leone A: Identification of reproducible individualized targets for treatment of depression with TMS based on intrinsic connectivity. Neuroimage 2013; 66:151–160

24. Kane G, Meade N: Ratio analysis using rank transformation. Review of Quantitative Finance and Accounting 1998; 10:59–74

25. O'Reardon JP, Solvason HB, Janicak PG, et al: Efficacy and safety of transcranial magnetic stimulation in the acute treatment of major depression: a multisite randomized controlled trial. Biol Psychiatry 2007; 62:1208–1216

26. Downar J, Geraci J, Salomons TV, et al: Anhedonia and reward-circuit connectivity distinguish nonresponders from responders to dorsomedial prefrontal repetitive transcranial magnetic stimulation in major depression. Biol Psychiatry 2014; 76:176–185

27. Dunlop K, Woodside B, Lam E, et al: Increases in frontostriatal connectivity are associated with response to dorsomedial repetitive transcranial magnetic stimulation in refractory binge/purge behaviors. Neuroimage Clin 2015; 8:611–618

28. Dunlop K, Woodside B, Olmsted M, et al: Reductions in cortico-striatal hyperconnectivity accompany successful treatment of obsessive-compulsive disorder with dorsomedial prefrontal rTMS. Neuropsychopharmacology 2016; 41:1395–1403

29. Padmanabhan JL, Cooke D, Joutsa J, et al: A human depression circuit derived from focal brain lesions. Biol Psychiatry 2019; 86: 749–758

30. Berlim MT, McGirr A, Beaulieu MM, et al: High frequency repetitive transcranial magnetic stimulation as an augmenting strategy in severe treatment-resistant major depression: a prospective 4-week naturalistic trial. J Affect Disord 2011; 130:312–317

31. Carpenter LL, Conelea C, Tyrka AR, et al: 5 Hz repetitive transcranial magnetic stimulation for posttraumatic stress disorder comorbid with major depressive disorder. J Affect Disord 2018; 235:414–420

32. Dilkov D, Hawken ER, Kaludiev E, et al: Repetitive transcranial magnetic stimulation of the right dorsal lateral prefrontal cortex in the treatment of generalized anxiety disorder: a randomized, double-blind sham controlled clinical trial. Prog Neuropsychopharmacol Biol Psychiatry 2017; 78:61–65

33. Leong K, Chan P, Grabovac A, et al: Changes in mindfulness following repetitive transcranial magnetic stimulation for mood disorders. Can J Psychiatry 2013; 58:687–691

34. Mansur CG, Myczkowki ML, de Barros Cabral S, et al: Placebo effect after prefrontal magnetic stimulation in the treatment of resistant obsessive-compulsive disorder: a randomized controlled trial. Int J Neuropsychopharmacol 2011; 14:1389–1397

35. Taylor SF, Ho SS, Abagis T, et al: Changes in brain connectivity during a sham-controlled, transcranial magnetic stimulation trial for depression. J Affect Disord 2018; 232:143–151

36. Tovar-Perdomo S, McGirr A, Van den Eynde F, et al: High frequency repetitive transcranial magnetic stimulation treatment for major depression: dissociated effects on psychopathology and neurocognition. J Affect Disord 2017; 217:112–117

37. Cusin C, Yang H, Yeung A, et al: Rating scales for depression. In Handbook of Clinical Rating Scales and Assessment in Psychiatry and Mental Health. Totowa, NJ, Humana Press, 2010, pp 7–35

38. Berlim MT, Van den Eynde F, Tovar-Perdomo S, et al: Augmenting antidepressants with deep transcranial magnetic stimulation (DTMS) in treatment-resistant major depression. World J Biol Psychiatry 2014; 15:570–578

39. Isserles M, Shalev AY, Roth Y, et al: Effectiveness of deep transcranial magnetic stimulation combined with a brief exposure procedure in post-traumatic stress disorder: a pilot study. Brain Stimul 2013; 6:377–383

40. Kaster TS, Daskalakis ZJ, Noda Y, et al: Efficacy, tolerability, and cognitive effects of deep transcranial magnetic stimulation for late-life depression: a prospective randomized controlled trial. Neuropsychopharmacology 2018; 43:2231–2238

41. Levkovitz Y, Harel EV, Roth Y, et al: Deep transcranial magnetic stimulation over the prefrontal cortex: evaluation of antidepressant and cognitive effects in depressive patients. Brain Stimul 2009; 2: 188–200

42. Rosenberg O, Shoenfeld N, Zangen A, et al: Deep TMS in a resistant major depressive disorder: a brief report. Depress Anxiety 2010; 27: 465–469

43. Rosenberg O, Zangen A, Stryjer R, et al: Response to deep TMS in depressive patients with previous electroconvulsive treatment. Brain Stimul 2010; 3:211–217

44. Tavares DF, Myczkowski ML, Alberto RL, et al: Treatment of bipolar depression with deep TMS: results from a double-blind, randomized, parallel group, sham-controlled clinical trial. Neuropsychopharmacology 2017; 42:2593–2601

45. Feighner JP: Nosology of primary affective disorders and application to clinical research. Acta Psychiatr Scand Suppl 1981; 290:29–41

46. Kennedy SH: Core symptoms of major depressive disorder: relevance to diagnosis and treatment. Dialogues Clin Neurosci 2008; 10: 271–277

47. Dombrovski AY, Blakesley-Ball RE, Mulsant BH, et al: Speed of improvement in sleep disturbance and anxiety compared with core mood symptoms during acute treatment of depression in old age. Am J Geriatr Psychiatry 2006; 14:550–554

48. van Loo HM, Cai T, Gruber MJ, et al: Major depressive disorder subtypes to predict long-term course. Depress Anxiety 2014; 31: 765–777

49. Pettorruso M, Martinotti G, Santacroce R, et al: rTMS reduces psychopathological burden and cocaine consumption in treatment-seeking subjects with cocaine use disorder: an open label, feasibility study. Front Psychiatry 2019; 10:621

50. Light SN, Bieliauskas LA, Taylor SF: Measuring change in anhedonia using the "Happy Faces" task pre- to post-repetitive transcranial magnetic stimulation (rTMS) treatment to left dorsolateral prefrontal cortex in major depressive disorder (MDD): relation to empathic happiness. Transl Psychiatry 2019; 9:217

51. Riva-Posse P, Choi KS, Holtzheimer PE, et al: Defining critical white matter pathways mediating successful subcallosal cingulate deep

brain stimulation for treatment-resistant depression. Biol Psychiatry 2014; 76:963–969

52. Kozak MJ, Cuthbert BN: The NIMH Research Domain Criteria initiative: background, issues, and pragmatics. Psychophysiology 2016; 53:286–297

53. Dinga R, Schmaal L, Penninx BWJH, et al: Evaluating the evidence for biotypes of depression: methodological replication and extension of Drysdale et al. (2017). Neuroimage Clin 2019; 22: 101796

54. Beck AT, Epstein N, Brown G, et al: An inventory for measuring clinical anxiety: psychometric properties. J Consult Clin Psychol 1988; 56:893–897

55. Opitz A, Fox MD, Craddock RC, et al: An integrated framework for targeting functional networks via transcranial magnetic stimulation. Neuroimage 2016; 127:86–96

56. Gordon EM, Laumann TO, Gilmore AW, et al: Precision functional mapping of individual human brains. Neuron 2017; 95: 791-807.e7

57. Fox MD, Snyder AZ, Vincent JL, et al: The human brain is intrinsically organized into dynamic, anticorrelated functional networks. Proc Natl Acad Sci USA 2005; 102:9673–9678

58. Choi KS, Riva-Posse P, Gross RE, et al: Mapping the "depression switch" during intraoperative testing of subcallosal cingulate deep brain stimulation. JAMA Neurol 2015; 72:1252–1260

59. Mayberg HS, Lozano AM, Voon V, et al: Deep brain stimulation for treatment-resistant depression. Neuron 2005; 45:651–660

60. Blumberger DM, Maller JJ, Thomson L, et al: Unilateral and bilateral MRI-targeted repetitive transcranial magnetic stimulation for treatment-resistant depression: a randomized controlled study. J Psychiatry Neurosci 2016; 41:E58–E66

61. Holtzheimer PE, Husain MM, Lisanby SH, et al: Subcallosal cingulate deep brain stimulation for treatment-resistant depression: a multisite, randomised, sham-controlled trial. Lancet Psychiatry 2017; 4:839–849

62. Dougherty DD, Rezai AR, Carpenter LL, et al: A randomized sham-controlled trial of deep brain stimulation of the ventral capsule/ventral striatum for chronic treatment-resistant depression. Biol Psychiatry 2015; 78:240–248

63. Fasano A, Daniele A, Albanese A: Treatment of motor and non-motor features of Parkinson's disease with deep brain stimulation. Lancet Neurol 2012; 11:429–442

64. Horn A, Reich M, Vorwerk J, et al: Connectivity predicts deep brain stimulation outcome in Parkinson disease. Ann Neurol 2017; 82:67–78